Detailed study of quark-hadron duality in spin structure functions of the proton and neutron

V. Lagerquist [1], S. E. Kuhn [1,*] and N. Sato [2]
[1] *Old Dominion University, Norfolk, Virginia 23529, USA*
[2] *Thomas Jefferson National Accelerator Facility, Newport News, Virginia 23606, USA*

(Received 6 May 2022; revised 21 November 2022; accepted 20 March 2023; published 6 April 2023)

Background: The response of hadrons, the bound states of the strong force (QCD), to external probes can be described in two different, complementary frameworks: as direct interactions with their fundamental constituents, quarks and gluons, or alternatively as elastic or inelastic coherent scattering that leaves the hadrons in their ground state or in one of their excited (resonance) states. The former picture emerges most clearly in hard processes with high momentum transfer, where the hadron response can be described by the perturbative expansion of QCD, while at lower energy and momentum transfers, the resonant excitations of the hadrons dominate the cross section. The overlap region between these two pictures, where both yield similar predictions, is referred to as quark-hadron duality and has been extensively studied in reactions involving unpolarized hadrons. Some limited information on this phenomenon also exists for polarized protons, deuterons, and ^{3}He nuclei, but not yet for neutrons.

Purpose: In this paper, we present comprehensive and detailed results on the correspondence between the extrapolated deep inelastic structure function g_1 of both the proton and the neutron with the same quantity measured in the nucleon resonance region. Thanks to the fine binning and high precision of our data, and using a well-controlled perturbative QCD (pQCD) fit for the partonic prediction, we can make quantitative statements about the kinematic range of applicability of both local duality and global duality.

Method: We use the most updated QCD global analysis results at high x from the Jefferson Lab Angular Momentum Collaboration to extrapolate the spin structure function g_1 into the nucleon resonance region and then integrate over various intervals in the scaling variable x. We compare the results with the large data set collected in the quark-hadron transition region by the CLAS Collaboration, including, for the first time, deconvoluted neutron data, integrated over the same intervals. We present this comparison as a function of the momentum transfer Q^2.

Results: We find that, depending on the integration interval and the minimum momentum transfer chosen, a clear transition to quark-hadron duality can be observed in both nucleon species. Furthermore, we show, for the first time, the approach to scaling behavior for g_1 measured in the resonance region at sufficiently high momentum transfer.

Conclusions: Our results can be used to quantify the deviations from the applicability of pQCD for data taken at moderate energies and can help with extraction of quark distribution functions from such data.

DOI: 10.1103/PhysRevC.107.045201

I. INTRODUCTION

QCD is the fundamental theory describing the interactions between quarks and gluons (partons), leading to their observed bound states (hadrons) and the strong nuclear force. At high spatial resolution (momentum scale), the QCD coupling constant becomes small (asymptotic freedom [1,2]), and quark and gluon interactions can be calculated perturbatively (pQCD). This leads to the emergence of these partons as effective degrees of freedom in the description of hard processes like deep inelastic scattering where the observed cross section can be described approximately as an incoherent sum of scattering cross sections on individual pointlike and structureless partons. On the other hand, at low momenta and long-distance scales, the interaction becomes strong and a perturbative treatment is no longer possible. Instead, physical processes can be best described in terms of effective hadronic degrees of freedom, e.g., the excitation of resonant hadronic states. By varying the resolution of a probe from short to long distances, physical cross sections display a transition from the partonic to the hadronic domains. It remains an important question whether there is a region where both pictures apply simultaneously, i.e., whether a parton-based description can reproduce the data in the kinematic region of hadronic resonances, at least on average. This phenomenon is known as quark-hadron duality [3–6]. While strong evidence for duality has been found, it is important to fully test the applicability of this concept in the case where spin degrees of freedom are present, and for different hadronic systems. If quark-hadron duality can be firmly established and its applicability quantitatively described, one can use measurements of hadronic

*Corresponding author: skuhn@odu.edu

 ©2023 American Physical Society

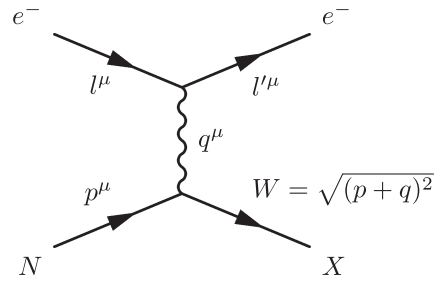

FIG. 1. Feynman diagram for inclusive electron scattering off a nucleon target. W is the invariant mass of the unobserved final-state X. All other symbols are explained in the text.

observables to improve contraints on the parton structure of these hadrons. For instance, measurements of nucleon structure functions that are sensitive to high parton momentum fraction x are very difficult at high energies, which limits our knowledge of the very important behavior of the underlying parton distribution functions (PDFs) as $x \to 1$. If the requirement of avoiding the region of nucleon resonances can be relaxed in a controlled manner, data taken at lower energies could contribute invaluable information on this asymptotic behavior.

In the present paper, we present new results on tests of duality in proton and neutron spin structure functions. Following this Introduction, we introduce the relevant formalism and theoretical concepts, describe the data set we analyzed as well as the phenomenologically extracted spin structure functions from the Jefferson Lab Angular Momentum (JAM) Collaboration QCD global analysis to which we compare these data, and then present results and conclusions.

II. THEORETICAL BACKGROUND

In this paper, we focus on quark-hadron duality in polarized inclusive electron scattering off polarized nucleon targets. In the single-photon-exchange approximation, an electron with four-momentum l scatters with final momentum l' from a nucleon with momentum p by exchanging a spacelike virtual photon with momentum $q = l - l'$ (see Fig. 1).

The invariant cross sections can then be written as [7]

$$E' \frac{d\sigma}{d^3 l'} = \frac{2\alpha^2}{sQ^4} L_{\mu\nu} W^{\mu\nu}, \tag{1}$$

where $Q^2 = -q^2$ is the virtuality of the exchanged photon, $L_{\mu\nu}$ is the leptonic tensor, and $W_{\mu\nu}$ is the hadronic tensor. The latter can be written as a linear combination of the unpolarized structure functions $F_{2,L}$ and the polarized structure functions $g_{1,2}$. The polarized structure functions can be experimentally accessed by measuring cross sections' differences of the form

$$d\sigma^{\downarrow\Uparrow} - d\sigma^{\uparrow\Uparrow}, \tag{2}$$

where $\downarrow\Uparrow$ and $\uparrow\Uparrow$ corresponds to antiparallel and parallel beam and target spin configurations, respectively.

In the kinematics of moderate $x = Q^2/2P \cdot q$ and Q^2 much larger than hadronic mass scales, the g_1 structure function can be approximated in collinear factorization schematically as

$$g_1(x, Q^2) = \sum_i \int_x^1 \frac{d\xi}{\xi} \Delta f_{i/N}(\xi, Q^2) \Delta H_i\left(\frac{x}{\xi}, \alpha_S(Q^2)\right) + O\left(\frac{m}{Q}\right). \tag{3}$$

Here the sum runs over all parton flavors i. The term ΔH_i is the target-independent short-distance partonic coefficient function calculable in pQCD in powers of the strong coupling constant α_S and is convoluted with the spin-dependent PDF Δf in the variable ξ. The factorization theorem is valid up to corrections of the order m/Q, where m is a generic hadronic mass scale. The ξ variable is the light-cone momentum fraction of partons relative to the parent hadron, i.e., $\xi = k^+/p^+$. At leading order in pQCD, the hard factor ΔH_i is proportional to $\delta(x - \xi)$; hence the structure function g_1 has a leading-order sensitivity to PDFs at $\xi = x$. Beyond the leading order, however, the physical structure function receives PDF contributions in the range $x < \xi < 1$ due to the convolution in Eq. (3). The scale dependence on Q^2 in Δf is governed by the Dokshitzer-Gribov-Lipatov-Altarelli-Parisi (DGLAP) [8–10] evolution equations stemming from the renormalization of parton densities and is given as

$$\frac{d\Delta f_i}{d\ln\mu^2}(\xi, \mu^2) = \sum_j \int_\xi^1 \frac{dy}{y} \Delta P_{ij}\left(\frac{\xi}{y}, \alpha_S(\mu^2)\right) \Delta f_j(y, \mu^2), \tag{4}$$

where ΔP_{ij} are the Altarelli-Parisi spacelike splitting functions. Finally we remark that the structure function g_2 has no leading power contribution.

Since the focus of our study is the behavior of g_1 in the large-x, moderate-Q^2 regime, it is important to utilize a QCD global analysis framework that has a maximal kinematical overlap in x to allow us to study duality with minimal extrapolation. In Ref. [11], the JAM Collaboration carried out a comprehensive analysis of the double-spin asymmetries in Deep Inelastic Scattering (DIS) with an extended kinematic coverage in x and Q^2 including data with a final-state mass as low as $W^2 = 4$ GeV^2. To our knowledge, this is the only global analysis that has included systematically all the high-x data from the CLAS Collaboration: 6 GeV with dedicated treatments for twist-3 effects and target mass corrections for the double-spin asymmetries. In the following, we utilize the inferred g_1 from the JAM Collaboration global analysis (which has a kinematic convergence up to $x \approx 0.7$) and use DGLAP backward evolution to access the resonance region at high x and lower Q^2.

For moderate final hadronic state masses, $W < 2$ GeV, the cross section typically exhibits multiple resonance peaks that appear when the target is excited into other baryonic states before later decaying into final-state products. This is illustrated in Fig. 2 for the F_2 structure function. This so-called resonance region can be best described in terms of hadronic degrees of freedom, where the cross section is expressed in terms of transition strengths to the various nucleon resonances, together with nonresonant hadron production contributions [12].

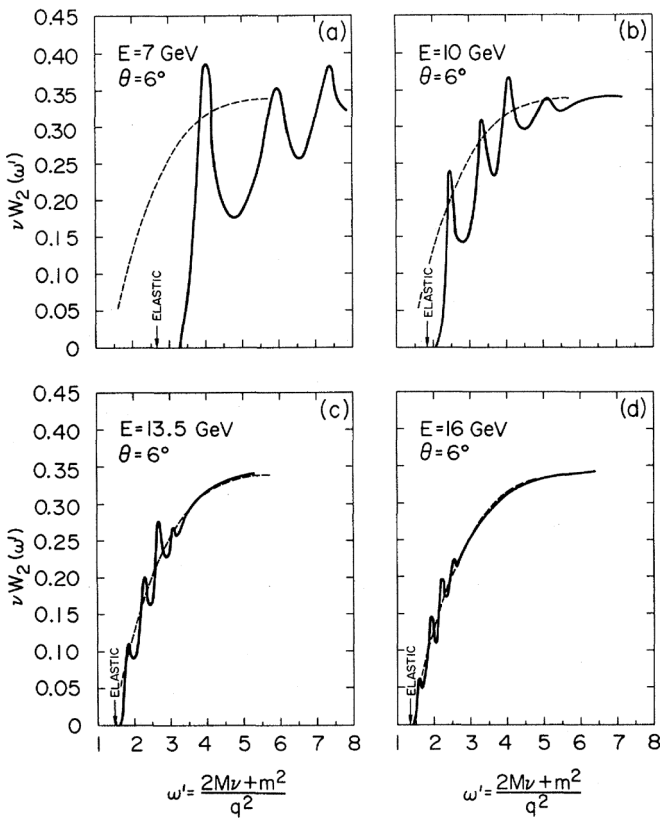

FIG. 2. Schematic dependence of the measured structure function F_2 in inelastic electron scattering off the nucleon on the variable $\omega' = W^2/Q^2 + 1$, which is close to $1/x$ at large Q^2. Panels (a) through (d) are for increasing four-momentum transfer Q^2. As can be observed, the resonance excitations of the nucleon are most prominent at low Q^2, while at higher Q^2 the curve for F_2 approaches the scaling limit (dashed line), hence indicating a transition to quark-hadron duality in this observable. Reproduced from the paper by Bloom and Gilman [3], with the permission of AIP Publishing.

It is not *a priori* obvious how this resonant behavior is related to the underlying degrees of freedom of all hadrons, quarks, and gluons, and their description in terms of PDFs, perhaps augmented by higher-twist terms in the Operator Product Expansion (OPE). This is addressed by the concept of quark-hadron duality that was first introduced in a publication by Bloom and Gilman in 1970 [3,4]. They found that the F_2 structure function measured in the nucleon resonance region approaches a smooth "scaling curve" as Q^2 increases, with the resonant troughs and peaks approximately averaging out to match an extrapolation of the deep inelastic structure function at high W into the resonance region (see Fig. 2).

In particular, Bloom and Gilman [3,4] proposed that integrals over specific ranges in $\omega' = 1/x + M^2/Q^2$ (or just over x) of either the extrapolated DIS fits or the experimental data in the resonance region would give similar results. The case where the limits of integration cover only 100–200 MeV on either side of a single resonance peak is referred to as local duality, as opposed to global duality which covers the entire resonance region from threshold to $W = 2$ GeV, potentially also including the elastic peak. In either case, the relation can be summarized as

$$\int_{x_1(W_1,Q^2)}^{x_2(W_2,Q^2)} dx\, F_2^{\rm res}(x,Q^2) = \int_{x_1}^{x_2} dx\, F_2^{\rm DIS}(x,Q^2), \qquad (5)$$

where $F_2^{\rm res}$ is the structure function measured over some kinematic range within the resonance region, between W_2 and W_1 (both below $W = 2$ GeV), while $F_2^{\rm DIS}$ is extrapolated from a QCD global analysis. Here,

$$x(W,Q^2) = \frac{Q^2}{W^2 - M^2 + Q^2}. \qquad (6)$$

Since the initial discovery by Bloom and Gilman [3] in 1970, considerable progress has been made in the measurement of unpolarized structure functions at low to moderate Q^2 and W and their interpretation in terms of quark-hadron duality, notably at the Thomas Jefferson National Accelerator Facility (also known as Jefferson Lab) [13–20].

In addition to this, spin-dependent structure functions in the same kinematic region have also been studied. Experiments at the Stanford Linear Accelerator Center (SLAC) in the late 1970s provided the first resonance region measurements for polarized proton-electron scattering [21,22]. These experiments hinted at the applicability of Bloom-Gilman duality to proton spin structure functions. They were followed in the 1990s by further experiments at SLAC by the E143 Collaboration, which expanded their g_1 and g_2 measurements to the resonance region [23,24]. In 2003, the HERMES Collaboration [25]) published their results specifically on the quark-hadron duality for the proton asymmetry A_1 measured at five different points in average x (corresponding to five different regions in average Q^2). These data, together with the E143 ones, were analyzed in a paper by Bianchi *et al.* [26] which contrasted, for the first time, the kinematic range where duality seemed to hold for unpolarized vs polarized structure functions. They were followed by data from Jefferson Lab (Hall B [27] and Hall A [28]) which contributed to the investigation of spin structure functions in the resonance region with increased kinematical coverage. Most of these early experiments had limited statistical precision and fairly few and wide bins. The new century brought additional high-precision experiments at Jefferson Lab (Hall A [29–33], Hall B [34–39], and Hall C [40]). Even for those, the neutron structure functions in the resonance region were extracted from measurements on nuclei without unfolding their smearing through nuclear Fermi motion. The present paper uses the most extensive data set available so far and for the first time includes unfolded spin structure functions of the neutron.

Studying quark-hadron duality in the spin sector is important, since polarization-dependent observables can have both positive and negative sign, and hence offer a more stringent test of duality For instance, it is well known that the transition to Δ baryons in the final state are dominated by the $M1$ amplitude, which should lead to a negative asymmetry A_1 and negative g_1. Meanwhile, given the rather low W of the lowest-lying $\Delta(1232)$, the extrapolated values for g_1 from pQCD fits will be at high values of x, where most DIS data indicate positive values for g_1.

In the present paper, we are presenting a new comparison of the most comprehensive data set on spin structure functions in the transition region between hadronic and partonic degrees of freedom, from the EG1b experiment [37,38] to the recent JAM Collaboration QCD global analysis [11] at high x. For the first time, we include the unfolded neutron structure function g_1 in this comparison. We address both the question of under what circumstances global and/or local duality holds and of what data from which kinematic region may be used to further constrain pQCD fits without introducing excessive higher-twist corrections.

III. INPUT DATA

For a detailed study of duality, one needs a dense set of data that cover the entire resonance region (conventionally from $W = 1.072$ to 2 GeV) in fine W bins, for a large number of bins in Q^2. The most comprehensive such data set was collected by the "EG1b" experiment carried out with the CEBAF Large Acceptance Spectrometer (CLAS) [41] at Jefferson Lab during 2000–2001 [34–38]. The experiment used the polarized electron beam from the Continuous wave Electron Beam Accelerator Facility (CEBAF) at Jefferson Lab, with beam energies of 1.6, 2.5, 4.2, and 5.7 GeV. Together with the large acceptance of CLAS, this set of beam energies yielded a large kinematic reach (with partially overlapping regions), covering nearly 2 orders of magnitude in Q^2 ($Q^2 = 0.06...5$) and W from threshold to about 3 GeV. A particular advantage of the wide acceptance of CLAS is that the data could be sorted into a predetermined grid of Q^2 and W, with no need to interpolate between different data points.

The polarized nucleon targets were provided in the form of irradiated frozen ammonia and deuterated ammonia for measurements of proton and deuteron asymmetries, respectively. The target was polarized through dynamic nuclear polarization and reached a polarization along the beam direction of approximately 75% for the protons and 30% for the deuterons [42].

The measured double-spin asymmetries were converted into spin structure functions $g_1(W, Q^2)$ using a phenomenological fit to the world data on polarized and unpolarized structure functions. In the case of the neutron structure function g_1^n, a folding prescription [43] was used to relate the measured spin structure function of the deuteron to g_1^n for each kinematic point. This yielded the first data set of unintegrated neutron spin structure functions in the resonance region. Details about the experiment, the data analysis and the complete data sets can be found in Refs. [37,38].

Extrapolated pQCD predictions for g_1^p and g_1^n, which are compared to the resonance region data in this paper, are taken from the JAM15 fits [11] of the world data on inclusive spin observables, including the EG1b data *outside* the resonance region (i.e., for $W > 2$ GeV). The JAM fits used a novel iterative Monte Carlo fitting method that utilizes data resampling techniques and cross-validation for a robust determination of the uncertainty band of the fitted PDFs as well as any observables predicted from the fit. A total of 2515 data points from 35 experiments and 4 facilities (CERN, SLAC, DESY, and JLab) were included in the fit.

TABLE I. Selected W Ranges, in GeV.

	Lower W limit	Upper W limit
1	1.072	1.38
2	1.38	1.58
3	1.58	1.82
4	1.82	2
5	1.072	2
6	0.939	2

IV. ANALYSIS

In this paper, we investigate two different but related tests of duality: (i) a direct comparison between truncated integrals over measured spin structure functions, each covering a specific range in the final-state mass W, and corresponding integrals over the extrapolated pQCD fits, and (ii) a study of the approach to scaling for g_1 averaged over a set of fixed narrow ranges in x.

For the first test, we select six different ranges of W as shown in Table I. The first four of these ranges cover specific prominent resonance peaks visible in inclusive unpolarized cross-section data (see Fig. 2): the Δ resonance [$\Delta(1232)3/2^+$], the region of the N(1440)$1/2^+$, N(1520)$3/2^-$, and N(1535)$1/2^-$ resonances, the region of the N(1680)$5/2^+$ and nearby resonances, and the remaining region up to $W = 2$ GeV, which does not exhibit a strong peak in the inclusive spin-averaged cross section but is known to contain several Δ resonances. We test whether local duality holds in each of these individual resonance regions. The next range (line 5 in Table I) covers the entire "canonical" resonance region, 1.072 GeV $< W <$ 2 GeV, i.e., the previous four regions combined. For the last range we add the elastic peak at $W = 0.939$ GeV, the nucleon mass, to cover the entire region 0.939 GeV $< W <$ 2 GeV, extending the corresponding x-range up to $x = 1$. This elastic contribution comes in the form

$$g_1^{\rm el} = \frac{1}{2}\frac{G_E G_M + \tau G_M^2}{1+\tau}\delta(x-1),$$

where $G_M = F_1 + F_2$ and $G_E = F_1 - \frac{Q^2}{4M^2}F_2$ are the magnetic and electric Sachs form factors [44]. The corresponding integrals for the JAM extrapolation are simply integrated up to $x = 1$, but do not contain an elastic contribution since they are based on DIS pQCD fits.

For each of these W ranges, our analysis process is the same. Experimental data for $g_1(x, Q^2)$ are first sorted into bins of Q^2 with limits shown in Table II (see Fig. 3). The W limits for each range are mapped to the corresponding values for x, following Eq. (6). The data are then integrated over the corresponding x-ranges to yield the truncated first moments of g_1,

$$\bar{\Gamma}_1(\Delta W, Q^2) = \int_{x_1(W_1,Q^2)}^{x_2(W_2,Q^2)} dx\, g_1(x, Q^2). \tag{7}$$

The corresponding truncated DIS integrals have been calculated by extrapolating the PDF fits of the JAM Collaboration to the central Q^2 value of each bin.

TABLE II. Experimental Q^2 Ranges, in GeV^2.

Lower Q^2	Upper Q^2	Central Q^2
0.92	1.10	1.00
1.10	1.31	1.20
1.31	1.56	1.43
1.56	1.87	1.71
1.87	2.23	2.04
2.23	2.66	2.43
2.66	3.17	2.91
3.17	3.79	3.47
3.79	4.52	4.14
4.52	5.40	4.94
5.40	6.45	5.90

For the experimental data, the statistical and experimental errors are added in quadrature into the integration and displayed with corresponding error bars. The integrals from the JAM fits are shown as bands corresponding to $\pm$ 1-σ CL.

For our second investigation, we define a sequence of fixed bins in x, each with a width of $\Delta x = 0.05$. The measured g_1 points are averaged within each of these x bins for each of the same Q^2 bins as before, and the averages are plotted against the nominal Q^2 values. Again, the JAM fits are treated in the same way and shown as bands together with the data. In this case, we show results both for the resonance region and beyond $W = 2$ GeV, depending on the x range.

V. RESULTS

In this section, we present the results of our two tests of duality. We begin by showing the truncated integrals $\bar{\Gamma}_1(\Delta W, Q^2)$ for both protons and neutrons over each of our six different ranges in W in Fig. 4. Figures 4(a)–(d) test local duality in each of the four ranges of prominent nucleon resonances, while Figs. 4(e) and 4(f) test global duality over the entire resonance region.

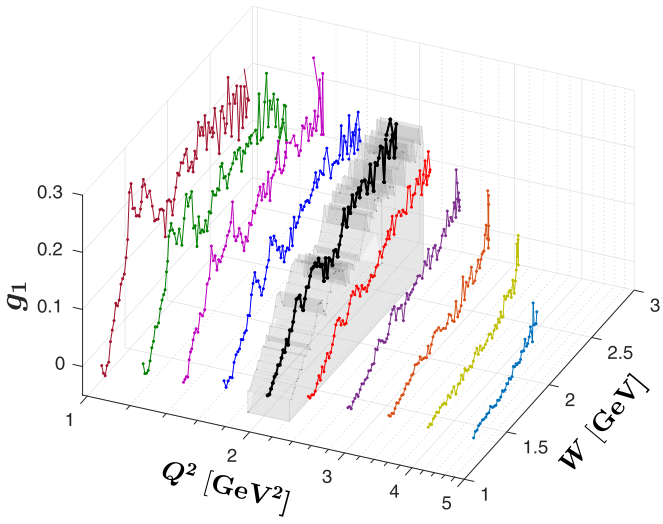

FIG. 3. Representation of the experimental data set used in this analysis. The measured data points are binned in bins in Q^2, as indicated by the shaded area for the example of the bin 1.87 GeV^2 < Q^2 < 2.23 GeV^2; see also Table II. The truncated integrals are then formed over specific regions in W as spelled out in Table I.

Figure 4(a) shows the truncated integrals over the region of the lowest-lying Δ resonance. It is clear that duality does not work very well in this region, especially for the proton (upper bands and data points). Both the proton and the neutron data are either negative (neutron, lower band and data points) or close to zero (proton), while the PDF extrapolation for both is positive (significantly so for the proton). This disagreement is due to the well-known fact that the excitation of the Δ resonance is dominated by a $M1$ transition, for which the final-state helicity 3/2 has a stronger coupling than the final-state helicity 1/2, leading to a negative (virtual) photon asymmetry A_1 and, in consequence, a negative value for g_1. Meanwhile, the relatively low value of W corresponds to large values of x, where most PDF fits predict a rising positive asymmetry. The JAM fit furthermore predicts a rather strong positive contribution from finite target mass and higher-twist effects (solid upper band), making the disagreements more pronounced. Convergence of the resonance region data towards the PDF extrapolation only begins around $Q^2 > 3$ GeV^2 for the neutron, and even later for the proton if the nonleading twist is included in the extrapolation. Consequently, local duality is not a good assumption for spin structure functions in the Δ region.

The next two resonance regions Figs. 4(b) and 4(c) show remarkably good agreement between the data and the extrapolated PDF bands (in particular the extrapolations including higher twist), indicating that "local duality" works well for these resonances. It may, therefore, be possible to include truncated integrals over these two regions in future PDF fits that include higher-twist contributions, helping to constrain these fits at high x where experimental data are scarce. The remaining region, up to $W = 2$ GeV, shows again a deviation of the data that tend to lie below the PDF fits. Once again, this is consistent with the assumption that this region has a strong contribution from various Δ-resonances, where the helicity-3/2 contribution dominates at small Q^2.

Finally, for a test of global duality, we integrate the data over the entire resonance region, 1.072 GeV < W < 2 GeV Fig. 4(e). We see that the data for the proton fall short of the extrapolated PDF results up to rather high $Q^2 > 3.5$GeV^2, and even higher for the band including higher twist. The neutron data have larger uncertainties, but also tend to lie consistently below the extrapolated PDF results. This finding indicates that the very slow approach towards duality in the two Δ-resonance regions spoils global duality, in contrast to the case of unpolarized structure functions of the proton. However, this picture changes drastically if the integral is extended all the way to $x = 1$, including the elastic peak in the data [0.938 GeV < W < 2 GeV, Fig. 4(f)]. It is remarkable how the negative deviations in the lowest and highest W regions (both populated by Δ resonances) are compensated by the inclusion of the elastic peak to get a rather rapid approach to global duality. For the proton a clear (and nontrivial) agreement between data and PDF prediction is observed, starting around

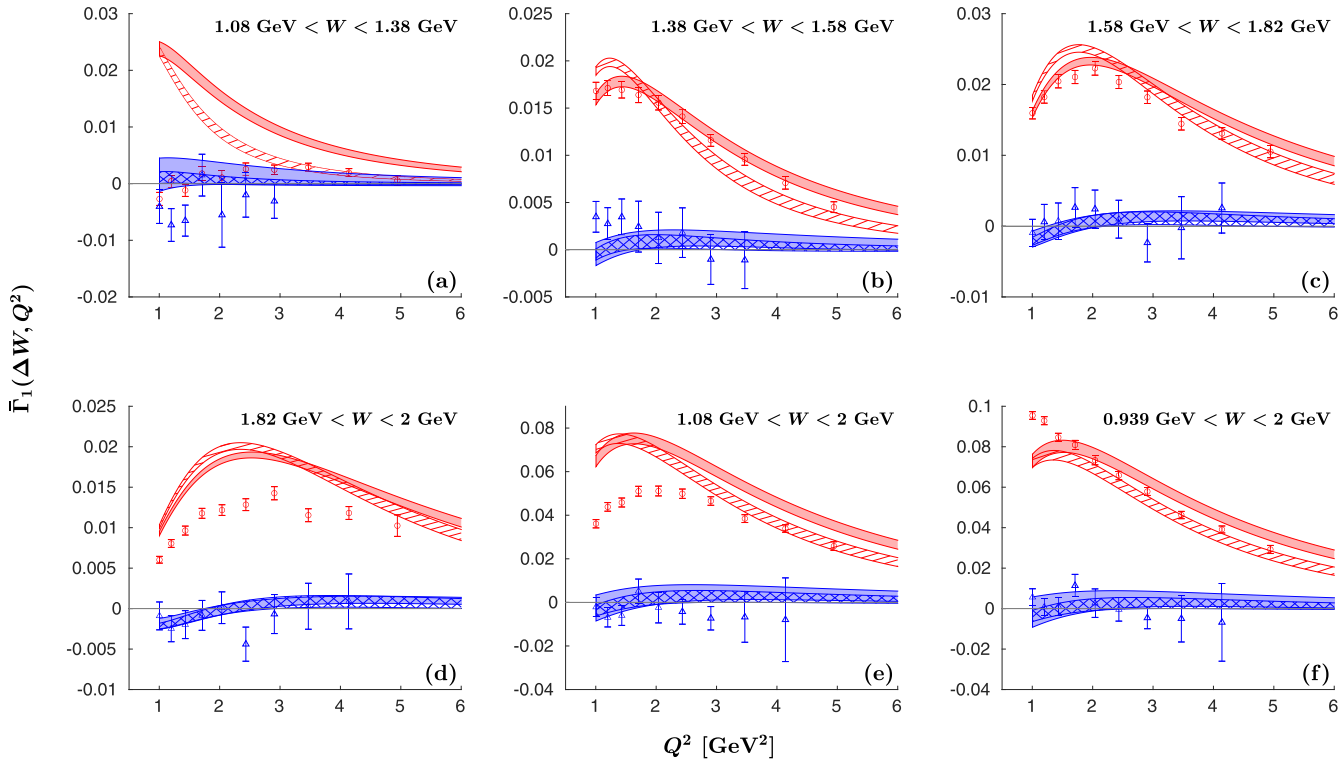

FIG. 4. Test of duality for truncated integrals. We show integrals $\bar{\Gamma}_1(\Delta W, Q^2)$ of the spin structure function $g_1(x, Q^2)$ over regions in x corresponding to six fixed regions ΔW of the final-state mass W, plotted as a function of Q^2. (a) The region of the first excited state of the nucleon, the $\Delta(1232)$ resonance. (b) The region of the $N(1440)1/2^+$, $N(1520)3/2^-$, and $N(1535)1/2^-$ resonances. (c) The region including the $N(1680)5/2^+$ resonance. (d) The remainder of the customary resonance region, 1.82 GeV $< W <$ 2 GeV. (e) The sum of regions in panels (a) through (d), i.e., the entire resonance region 1.07 GeV $< W <$ 2 GeV. (f) Same as panel (e), with the elastic peak included: 0.938 GeV $< W <$ 2 GeV (corresponding to a range in x extending all the way to $x = 1$). The top (red) bands and data points (circles) are for the proton, and the bottom (blue) bands and data points (triangles) are for the neutron. The data points are shown with statistical and systematic uncertainties added in quadrature (error bars). The solid bands show the full prediction from the extrapolated JAM fit, including target mass and higher-twist contributions. The striped band (proton) and the cross-hatched band (neutron) show the results including only the leading-twist contribution.

$Q^2 = 1.4$ GeV^2. For the neutron the predictions from the PDF fits as well as the data are mostly consistent with zero. There may be a slight tendency for the data to fall below zero at high Q^2, which would agree with the observation that the d-quark polarization appears to remain negative up to the highest x measured so far [29]. Overall, the integral over the entire resonance region can provide another constraint for future polarized PDF fits, *provided* the elastic peak is included in the integral.

In our second analysis, we are averaging the EG1b data and JAM PDF fits over fixed intervals in x for each of our Q^2 bins, to study the approach towards scaling for this averaged structure function $g_1(x, Q^2)$. The data and JAM predictions are integrated over bins of width $\Delta x = 0.05$ and then divided by Δx to obtain the average $\langle g_1 \rangle$. They are then multiplied by the bin centroid in x for better visibility (see Fig. 5). In contrast to the previous analysis, we include in these figures *all* data from EG1b, from both the resonance and the DIS region, with the boundary between the two indicated by the vertical dashed line at $Q^2 = (W^2_{\rm limit} - m^2)/(1/x - 1)$, with $W_{\rm limit} = 2$ GeV. The last panel in Fig. 5 shows all of the EG1b data points, with the gray band indicating the range of data points integrated over for a sample x-bin. For the first x-bin [Fig. 5(a)], all data points are already above the resonance region ($W > 2$ GeV) and show reasonably flat Q^2 dependence, albeit slightly below the fit to all world data.

For the next seven x-bins [Figs. 5(b)–(h)], some nontrivial structure can be seen just to the left of the boundary at $W = 2$ GeV, while the data at both higher and lower Q^2 [but above the $\Delta(1232)$ resonance region] seem to agree with the Q^2 behavior predicted by the extrapolated pQCD fit. These "dips" occur in the higher-lying resonance region where we already observed a slow convergence to the scaling limit, due to the presence of some Δ resonances. Finally, at the highest x-bins in our sample (bottom row), the data seem to converge more quickly towards the extrapolated pQCD fit, even far away from the $W = 2$ GeV limit [for the Figs. 5(j) and 5(k), *all* data are in the resonance region]. In this higher-x region, an approach to scaling is observed above $Q^2 = 3$ GeV^2, basically as soon as W is safely above the region of the $\Delta(1232)$ region. Thus, it appears as if the approach to scaling may begin early at larger x values, which would be very beneficial for the goal

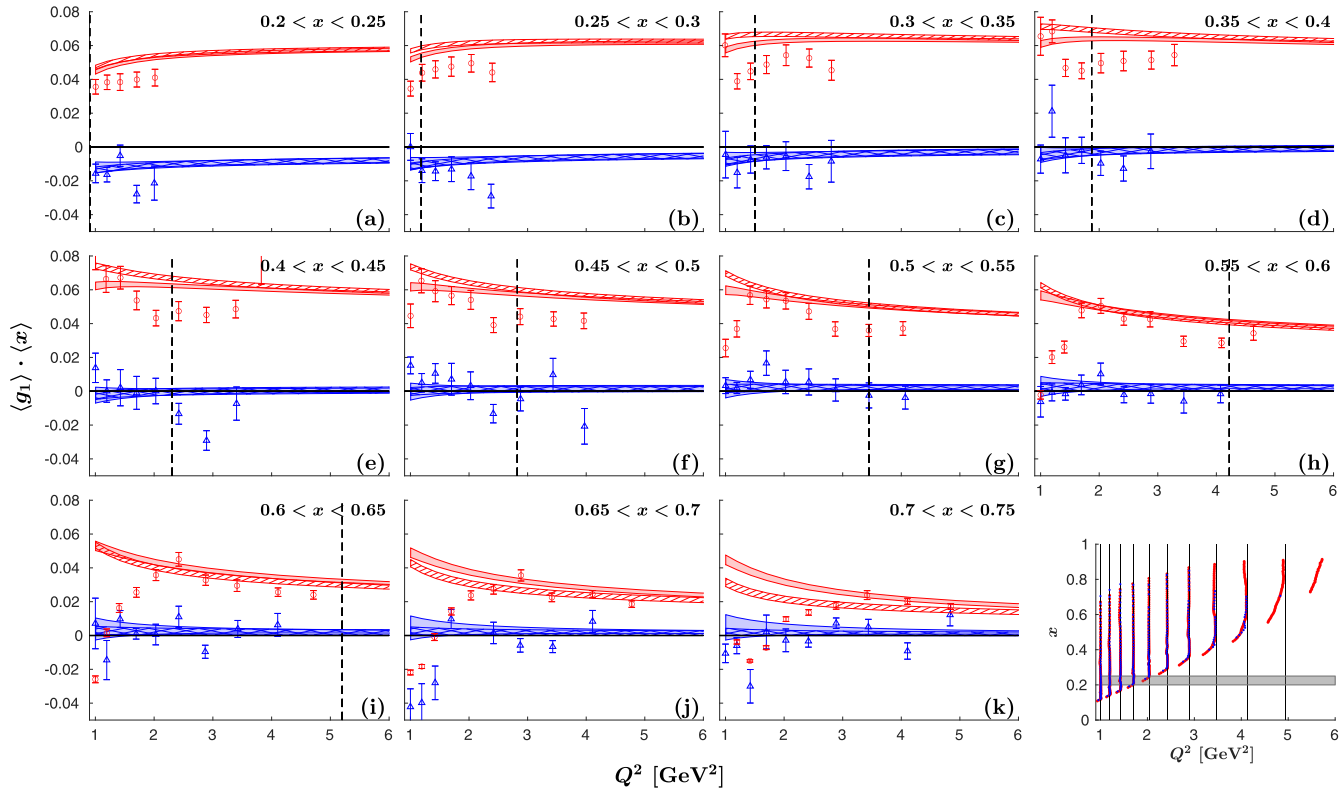

FIG. 5. Approach towards the scaling limit for the structure function $g_1(x, Q^2)$, averaged over 11 different x bins of width $\Delta x = 0.05$, as a function of Q^2. Data and JAM bands are shown multiplied with the average x for each bin for better clarity; symbols are the same as those in Fig. 4. The vertical dashed line indicates the limit $W = 2$ GeV of the resonance region, which lies to the left. Last panel: Kinematic location of all data points from EG1b in the x vs Q^2 plane [red, proton; blue, neutron). The gray band indicates a sample interval in x over which the data are averaged [corresponding to panel (a)], and the vertical lines indicate the nominal central values of each Q^2 bin.

of extracting the behavior of spin structure functions at large x, a topic of continuing high interest [45]. For tables for all data shown in Figs. 4 and 5, see the Supplemental Material [46].

VI. CONCLUSION

In this paper, we present the most detailed study of quark-hadron duality in the spin structure function g_1 to date, for both the proton and, for the first time, the neutron. We study several different formulations of duality and find that duality seems to hold much better (at smaller momentum transfer) in some cases than in others. In particular, we conclude the following.

(i) When forming integrals over kinematic regions corresponding to specific resonance peaks, we observe good agreement between the measured data and the extrapolation from pQCD fits whenever several resonances with different spins contribute, i.e., for the regions $W = 1.38$ to 1.58 GeV (including the N(1440)$1/2^+$, N(1520)$3/2^-$, and N(1535)$1/2^-$ resonances) and $W = 1.58$ to 1.82 GeV (several higher-lying resonances). In contrast, in the region dominated by the ground-state Δ resonance ($W = 1.08$ to 1.38 GeV) and the region $W = 1.82$ to 2 GeV with several Δ resonances, we observe a much slower approach of the measured integrals towards the extrapolated PDF fits with Q^2. This is likely due to the fact that, at least at moderately low Q^2, for the excitation of Δ resonances the transition to the final-state helicity 3/2 dominates.

(ii) If we integrate over the entire resonance region up to $W = 2$, including the elastic peak at $W = 0.938$ GeV, a rather rapid convergence towards the extrapolated PDF fits is observed: Global duality seems to work in spin structure functions. However, excluding the elastic peak leads to rather slow convergence of the truncated integral to the extrapolated pQCD expectation, due to the outsized influence of the negative contribution from the $\Delta(1232)$ resonance.

(iii) If instead we integrate over fixed bins in x, with different resonances contributing at different Q^2, we find that for lower values of x, the transition with Q^2 towards a smooth scaling curve occurs only if the value of Q^2 is high enough so that $W > 2$ GeV. Conversely, for the highest x values, we observe that the approach towards a smooth scaling curve (and the extrapolated PDF fits) occurs even below $W = 2$ GeV, albeit at a higher $Q^2 \approx 3$ GeV^2. This may be due to

the fact that at higher Q^2, resonant and nonresonant contributions with different asymmetries average out, leading to a "precocious" approach to scaling (or a different form of local duality). This observation supports the idea that, for high enough x and Q^2, even data in the resonance region may be used to constrain (polarized) parton distribution functions. Being able to include data in the resonance region and *a fortiori* at moderate $W^2 < 10$ GeV^2—a limit often imposed on PDF fits—will help with the goal to pin down more precisely the quark polarization of both types of valence quarks in the limit $x \to 1$, which is still an open question at this time.

ACKNOWLEDGMENTS

We would like to thank our collaborators on CLAS experiment EG1b and the members of the JAM Collaboration for their help with the analysis presented. We are particularly indebted to W. Melnitchouk for his valuable comments and to J. Ethier, who provided us with the extrapolated JAM results. We are grateful to the late Robert Fersch who provided the entire EG1b proton data set for our analysis. This work was supported by the DOE, Office of Science, Office of Nuclear Physics under Contract No. DE-FG02-96ER40960 (ODU). The work of N.S. was supported by the DOE, Office of Science, Office of Nuclear Physics, in the Early Career Program.

[1] D. J. Gross and F. Wilczek, Ultraviolet Behavior of Non-Abelian Gauge Theories, Phys. Rev. Lett. **30**, 1343 (1973).
[2] H. Politzer, Reliable Perturbative Results for Strong Interactions?, Phys. Rev. Lett. **30**, 1346 (1973).
[3] E. D. Bloom and F. J. Gilman, Scaling, Duality, and the Behavior of Resonances in Inelastic Electron-Proton Scattering, Phys. Rev. Lett. **25**, 1140 (1970).
[4] E. D. Bloom and F. J. Gilman, Scaling and the behavior of nucleon resonances in inelastic electron-nucleon scattering, Phys. Rev. D **4**, 2901 (1971).
[5] A. De Rujula, H. Georgi, and H. Politzer, Demythification of electroproduction, local duality and precocious scaling, Ann. Phys. **103**, 315 (1977).
[6] W. Melnitchouk, R. Ent, and C. Keppel, Quark-hadron duality in electron scattering, Phys. Rep. **406**, 127 (2005).
[7] J. Collins, *Foundations of Perturbative QCD* (Cambridge University, Cambridge, England, 2013), Vol. 32.
[8] Y. L. Dokshitzer, Calculation of the structure functions for deep inelastic scattering and $e^+ e^-$ annihilation by perturbation theory in quantum chromodynamics, Sov. Phys. JETP **46**, 641 (1977).
[9] V. Gribov and L. Lipatov, Deep inelastic e p scattering in perturbation theory, Sov. J. Nucl. Phys. **15**, 438 (1972).
[10] G. Altarelli and G. Parisi, Asymptotic freedom in parton language, Nucl. Phys. B **126**, 298 (1977).
[11] N. Sato, W. Melnitchouk, S. E. Kuhn, J. J. Ethier, and A. Accardi (Jefferson Lab Angular Momentum Collaboration), Iterative Monte Carlo analysis of spin-dependent parton distributions, Phys. Rev. D **93**, 074005 (2016).
[12] A. N. Hiller Blin *et al.*, Nucleon resonance contributions to unpolarized inclusive electron scattering, Phys. Rev. C **100**, 035201 (2019).
[13] I. Niculescu *et al.*, Experimental Verification of Quark Hadron Duality, Phys. Rev. Lett. **85**, 1186 (2000).
[14] I. Niculescu *et al.*, Evidence for Valencelike Quark Hadron Duality, Phys. Rev. Lett. **85**, 1182 (2000).
[15] M. Osipenko *et al.* (CLAS Collaboration), A Kinematically complete measurement of the proton structure function F_2 in the resonance region and evaluation of its moments, Phys. Rev. D **67**, 092001 (2003).
[16] I. Niculescu *et al.*, Direct observation of quark-hadron duality in the free neutron F_2 structure function, Phys. Rev. C **91**, 055206 (2015).
[17] M. E. Christy and P. E. Bosted, Empirical fit to precision inclusive electron-proton cross- sections in the resonance region, Phys. Rev. C **81**, 055213 (2010).
[18] V. Tvaskis *et al.*, Measurements of the separated longitudinal structure function F_L from hydrogen and deuterium targets at low Q^2, Phys. Rev. C **97**, 045204 (2018).
[19] S. P. Malace *et al.*, Applications of quark-hadron duality in F_2 structure function, Phys. Rev. C **80**, 035207 (2009).
[20] S. P. Malace, Y. Kahn, W. Melnitchouk, and C. E. Keppel, Confirmation of Quark-Hadron Duality in the Neutron F_2 Structure Function, Phys. Rev. Lett. **104**, 102001 (2010).
[21] G. Baum *et al.*, Measurement of Asymmetry in Spin-Dependent $e - p$ Resonance-Region Scattering, Phys. Rev. Lett. **45**, 2000 (1980).
[22] G. Baum *et al.*, New Measurement of Deep Inelastic $e - p$ Asymmetries, Phys. Rev. Lett. **51**, 1135 (1983).
[23] P. L. Anthony *et al.* (E142 Collaboration), Determination of the Neutron Spin Structure Function, Phys. Rev. Lett. **71**, 959 (1993).
[24] K. Abe *et al.* (E143 Collaboration), Measurements of the proton and deuteron spin structure functions g_1 and g_2, Phys. Rev. D **58**, 112003 (1998).
[25] A. Airapetian *et al.* (HERMES Collaboration), Evidence for Quark Hadron Duality in the Proton Spin Asymmetry A_1, Phys. Rev. Lett. **90**, 092002 (2003).
[26] N. Bianchi, A. Fantoni, and S. Liuti, Parton-hadron duality in unpolarized and polarized structure functions, Phys. Rev. D **69**, 014505 (2004).
[27] J. Yun *et al.* (CLAS Collaboration), Measurement of inclusive spin structure functions of the deuteron, Phys. Rev. C **67**, 055204 (2003).
[28] Z. E. Meziani *et al.*, Higher twists and color polarizabilities in the neutron, Phys. Lett. B **613**, 148 (2005).
[29] X. Zheng *et al.* (Jefferson Lab Hall A Collaboration), Precision measurement of the neutron spin asymmetries and spin-dependent structure functions in the valence quark region, Phys. Rev. C **70**, 065207 (2004).
[30] X. Zheng *et al.* (Jefferson Lab Hall A Collaboration), Precision Measurement of the Neutron Spin Asymmetry A_1^n and Spin Flavor Decomposition in the Valence Quark Region, Phys. Rev. Lett. **92**, 012004 (2004).

[31] P. Solvignon *et al.* (Jefferson Lab E01-012 Collaboration), Quark-Hadron Duality in Neutron (^{3}He) Spin Structure, Phys. Rev. Lett. **101**, 182502 (2008).

[32] D. S. Parno *et al.* (Jefferson Lab Hall A Collaboration), Precision measurements of A_1^n in the deep inelastic regime, Phys. Lett. B **744**, 309 (2015).

[33] D. Flay *et al.* (Jefferson Lab Hall A Collaboration), Measurements of d_2^n and A_1^n: Probing the neutron spin structure, Phys. Rev. D **94**, 052003 (2016).

[34] K. V. Dharmawardane *et al.* (CLAS Collaboration), Measurement of the x- and Q^2-dependence of the asymmetry A_1 on the nucleon, Phys. Lett. B **641**, 11 (2006).

[35] Y. Prok *et al.* (CLAS Collaboration), Moments of the spin structure functions g_1^p and g_1^d for $0.05 < Q^2 < 3.0\,\mathrm{GeV}^2$, Phys. Lett. B **672**, 12 (2009).

[36] P. E. Bosted *et al.* (CLAS Collaboration), Quark-hadron duality in spin structure functions g_1^p and g_1^d, Phys. Rev. C **75**, 035203 (2007).

[37] N. Guler *et al.* (CLAS Collaboration), Precise determination of the deuteron spin structure at low to moderate Q^2 with CLAS and extraction of the neutron contribution, Phys. Rev. C **92**, 055201 (2015).

[38] R. Fersch *et al.* (CLAS Collaboration), Determination of the proton spin structure functions for $0.05 < Q^2 < 5\,\mathrm{GeV}^2$ using CLAS, Phys. Rev. C **96**, 065208 (2017).

[39] R. G. Fersch (CLAS Collaboration), Quark-hadron duality of spin structure functions in CLAS EG1b data, Few-Body Syst. **59**, 108 (2018).

[40] F. R. Wesselmann *et al.* (Resonance Spin Structure Collaboration), Proton Spin Structure in the Resonance Region, Phys. Rev. Lett. **98**, 132003 (2007).

[41] B. A. Mecking *et al.* (CLAS Collaboration), The CEBAF large acceptance spectrometer (CLAS), Nucl. Instrum. Methods Phys. Res. Sect. A **503**, 513 (2003).

[42] C. D. Keith *et al.*, A polarized target for the CLAS detector, Nucl. Instrum. Methods Phys. Res. Sect. A **501**, 327 (2003).

[43] Y. Kahn, W. Melnitchouk, and S. A. Kulagin, New method for extracting neutron structure functions from nuclear data, Phys. Rev. C **79**, 035205 (2009).

[44] R. C. Walker *et al.*, Measurements of the proton elastic form-factors for $1 \leqslant Q^2 \leqslant 3\,(\mathrm{GeV}/c)^2$ at SLAC, Phys. Rev. D **49**, 5671 (1994).

[45] T. Liu, R. S. Sufian, G. F. de Téramond, H. G. Dosch, S. J. Brodsky, and A. Deur, Unified Description of Polarized and Unpolarized Quark Distributions in the Proton, Phys. Rev. Lett. **124**, 082003 (2020).

[46] See Supplemental Material at http://link.aps.org/supplemental/10.1103/PhysRevC.107.045201 for tables for all data points shown in this paper.